Auxiliary Material for

# Interdecadal Shifts of ENSO Influences on Spring Central Asian Precipitation

Mengyuan Yao[1,3], Haosu Tang[1,4], Gang Huang[1,3], Renguang Wu[2]

[1]*State key Laboratory of Numerical Modeling for Atmospheric Sciences and Geophysical Fluid Dynamics (LASG), Institute of Atmospheric Physics, Chinese Academy of Sciences, Beijing, China*

[2]*School of Earth Sciences, Zhejiang University, Hangzhou, China*

[3]*University of Chinese Academy of Sciences, Beijing, China*

[4]*Department of Geography, University of Sheffield, Sheffield, UK*

## Contents of this file

1. Supplementary Table 1
2. Supplementary Table 2
3. Supplementary Fig.1
4. Supplementary Fig.2
5. Supplementary Fig.3
6. Supplementary Fig.4
7. Supplementary Fig.5
8. Supplementary Fig.6

**Supplementary Table 1.** Details of 45 CMIP6 models used in this study.

| Model name | Atmospheric Resolution (latitude × longitude) | Institute |
|---|---|---|
| ACCESSCM2 | 1.25°×1.875° | CSIRO-BOM/Australia |
| ACCESS-ESM1-5 | 1.24°×1.875° | CSIRO-BOM/Australia |
| BCC-CSM2-MR | 1.125°×1.125° | BCC-CMA/China |
| BCC-ESM1 | 2.81°×2.81° | BCC-CMA/China |
| CAMS-CSM1-0 | 1.125°×1.125° | CAMS/China |
| CanESM5-CanOE | 2.81°×2.81° | CCCma/Canada |
| CanESM5 | 2.81°×2.81° | CCCma/Canada |
| CESM2-FV2 | 1.875°×2.5° | NSF-DOE-NCAR/United States |
| CESM2-WACCM-FV2 | 1.875°×2.5° | NSF-DOE-NCAR/United States |
| CESM2-WACCM | 0.94°×1.25° | NSF-DOE-NCAR/United States |
| CESM2 | 0.94°×1.25° | NSF-DOE-NCAR/United States |
| CNRM-CM6-1-HR | 0.5°×0.5° | CNRM-CERFACS/France |
| CNRM-CM6-1 | 1.4°×1.4° | CNRM-CERFACS/France |
| CNRM-ESM2-1 | 1.4°×1.4° | CNRM-CERFACS/France |
| E3SM-1-0 | 1°×1° | E3SM-Project/United States |
| E3SM-1-1-ECA | 1°×1° | E3SM-Project/United States |
| E3SM-1-1 | 1°×1° | E3SM-Project/United States |
| EC-Earth3-Veg | 0.7°×0.7° | EC-Earth-Consortium |
| EC-Earth3 | 0.7°×0.7° | EC-Earth-Consortium |
| FGOALS-f3-L | 1°×1.25° | LASG-CESS/China |
| FGOALS-g3 | 2.25°×2° | LASG-CESS/China |
| GFDL-CM4 | 1°×1.25° | NOAA-GFDL/United States |
| GFDL-ESM4 | 1°×1.25° | NOAA-GFDL/United States |
| GISS-E2-1-G-CC | 2°×2.5° | NASA-GISS/United States |
| GISS-E2-1-G | 2°×2.5° | NASA-GISS/United States |
| GISS-E2-1-H | 2°×2.5° | NASA-GISS/United States |

| | | |
|---|---|---|
| HadGEM3-GC31-LL | 1.25°×1.875° | MOHC/United Kingdom |
| HadGEM3-GC31-MM | 0.56°×0.83° | MOHC/United Kingdom |
| INM-CM4-8 | 1.5°×2° | INM/Russia |
| INM-CM5-0 | 1.5°×2° | INM/Russia |
| IPSL-CM6A-LR | 1.26°×2.5° | IPSL/France |
| KACE-1-0-G | 1.25°×1.875° | NIMS-KMA/Korea |
| MCM-UA-1-0 | 2.25°×3.75° | UA/United States |
| MIROC-ES2L | 2.81°×2.81° | MIROC/Japan |
| MIROC6 | 1.4°×1.4° | MIROC/Japan |
| MPI-ESM-1-2-HAM | 1.875°×1.875° | HAMMOZ-Consortium |
| MPI-ESM1-2-HR | 0.94°×0.94° | DKRZ/Germany |
| MPI-ESM1-2-LR | 1.875°×1.875° | MPI -M/Germany |
| MRI-ESM2-0 | 1.125°×1.125° | MRI/Japan |
| NESM3 | 1.875°×1.875° | NUIST/China |
| NorCPM1 | 1.875°×2.5° | NCC-NMI/Norway |
| NorESM2-LM | 1.875°×2.5° | NCC-NMI/Norway |
| NorESM2-MM | 0.94°×1.25° | NCC-NMI/Norway |
| SAM0-UNICON | 0.94°×1.25° | SUU/Korea |
| UKESM1-0-LL | 1.25°×1.875° | MOHC/United Kingdom |

**Supplementary Table 2**. Spatial correlations with observations in the whole period and in the HC period, and the difference between the maximum and minimum 19-yr sliding correlation coefficients.

| | **Spatial correlation** | **Spatial correlation in HC** | **Difference (max-min)** |
|---|---|---|---|
| OBS | 1 | 1 | 0.87 |
| ACCESS-CM2 | 0.52 | 0.27 | 0.34 |
| ACCESS-ESM1-5 | 0.53 | 0.44 | 0.86 |
| BCC-CSM2-MR | 0.08 | 0.09 | 1.09 |
| BCC-ESM1 | 0.47 | 0.49 | 1.13 |
| CAMS-CSM1-0 | -0.43 | -0.09 | 0.70 |
| CanESM5 | 0.44 | 0.21 | 0.74 |
| CanESM5-CanOE | 0.35 | 0.18 | 1.05 |
| CESM2 | 0.64 | 0.27 | 0.95 |
| CESM2-FV2 | 0.55 | 0.21 | 0.69 |
| CESM2-WACCM | 0.66 | 0.35 | 0.64 |
| CESM2-WACCM-FV2 | 0.49 | 0.12 | 0.72 |
| CNRM-CM6-1 | 0.51 | 0.45 | 0.62 |
| CNRM-CM6-1-HR | 0.58 | 0.46 | 1.20 |
| CNRM-ESM2-1 | -0.23 | 0.55 | 0.70 |
| E3SM-1-0 | -0.22 | 0.47 | 0.68 |
| E3SM-1-1 | 0.05 | 0.16 | 0.88 |
| E3SM-1-1-ECA | 0.63 | 0.43 | 0.74 |
| EC-Earth3 | -0.52 | -0.20 | 0.57 |
| EC-Earth3-Veg | 0.71 | 0.44 | 0.73 |
| FGOALS-f3-L | 0.20 | -0.26 | 0.68 |
| FGOALS-g3 | 0.66 | 0.25 | 0.42 |
| GFDL-CM4 | 0.56 | 0.03 | 0.84 |
| GFDL-ESM4 | 0.04 | 0.09 | 0.76 |
| GISS-E2-1-G | 0.69 | 0.48 | 0.66 |
| GISS-E2-1-G-CC | 0.57 | -0.11 | 0.68 |
| GISS-E2-1-H | 0.63 | 0.35 | 0.59 |
| HadGEM3-GC31-LL | 0.57 | 0.34 | 0.98 |
| HadGEM3-GC31-MM | 0.63 | 0.54 | 0.93 |
| INM-CM4-8 | 0.40 | 0.32 | 0.81 |
| INM-CM5-0 | 0.28 | 0.24 | 1.33 |
| IPSL-CM6A-LR | 0.35 | 0.12 | 0.85 |
| KACE-1-0-G | 0.47 | 0.14 | 0.71 |
| MCM-UA-1-0 | 0.53 | 0.17 | 0.91 |
| MIROC6 | 0.62 | 0.41 | 0.69 |
| MIROC-ES2L | 0.63 | 0.39 | 0.44 |
| MPI-ESM-1-2-HAM | 0.39 | 0.24 | 0.96 |
| MPI-ESM1-2-HR | 0.50 | 0.47 | 0.95 |

| | | | |
|---|---|---|---|
| MPI-ESM1-2-LR | -0.01 | 0.40 | 0.88 |
| MRI-ESM2-0 | 0.56 | 0.38 | 0.66 |
| NESM3 | 0.55 | 0.41 | 0.88 |
| NorCPM1 | 0.57 | 0.07 | 1.04 |
| NorESM2-LM | 0.55 | 0.45 | 0.62 |
| NorESM2-MM | 0.56 | 0.08 | 0.80 |
| SAM0-UNICON | 0.67 | 0.58 | 0.92 |
| UKESM1-0-LL | 0.74 | 0.62 | 0.77 |

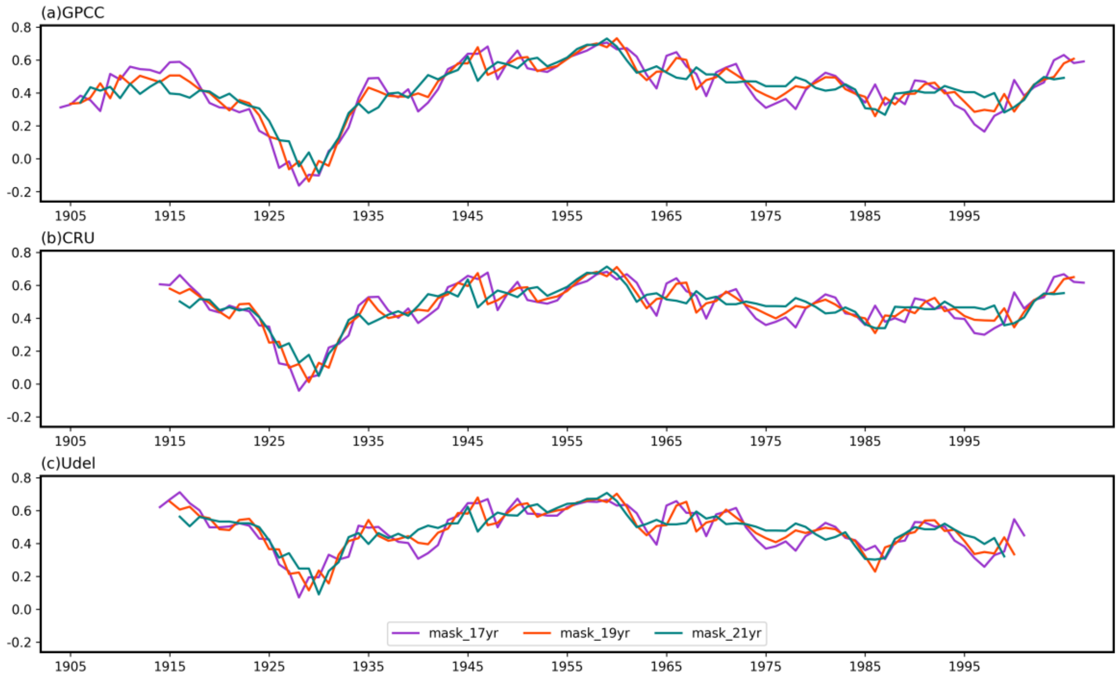


**Supplementary Fig. 1 Response of precipitation (unit: mm/day) to El Niño in different datasets and window length.** The 17-yr, 19-yr and 21-yr sliding correlation of the precipitation over CA with normalized DJF(0) Niño3.4 index in (a) GPCC, (b) CRU, and (c) Udel dataset.

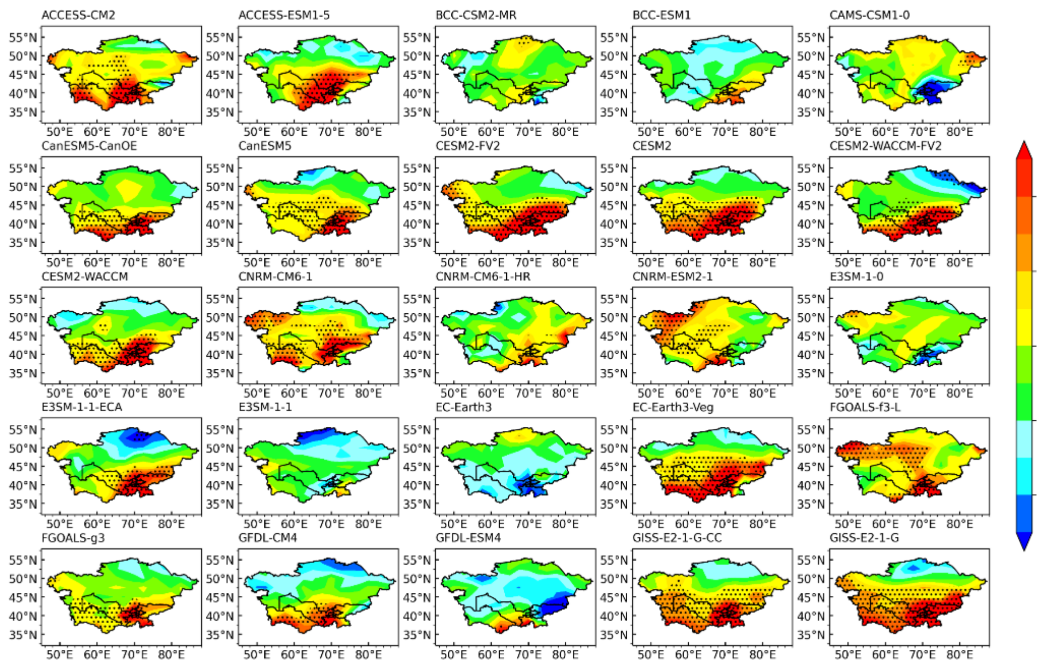


**Supplementary Fig. 2 Spatial response of precipitation (unit: mm/day) to El Niño.** Regression of the MAM(1) precipitation over CA with normalized DJF(0) Niño3.4 index for historical experiments of 45 CMIP6 models.

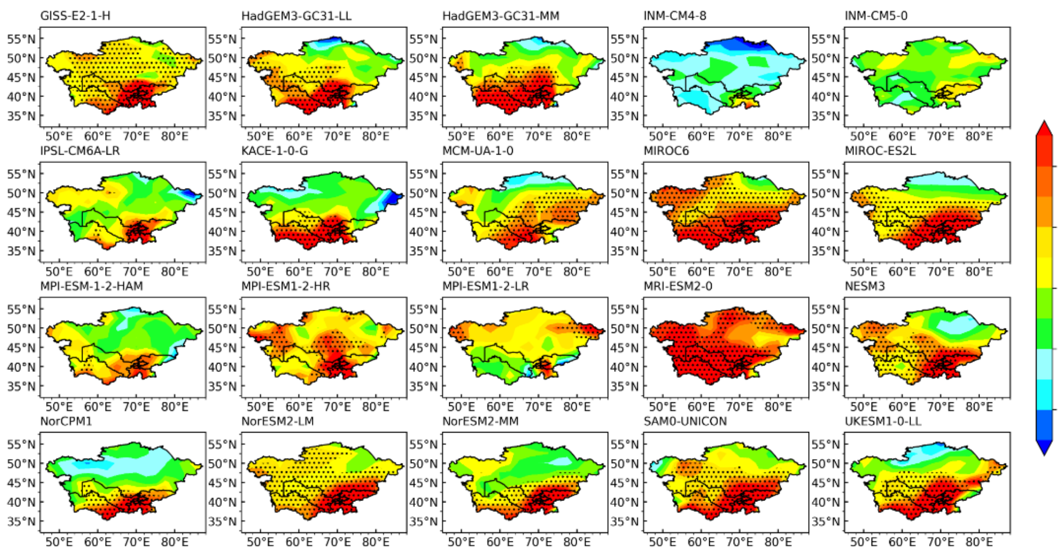


**Continued** Supplementary Fig. 2.

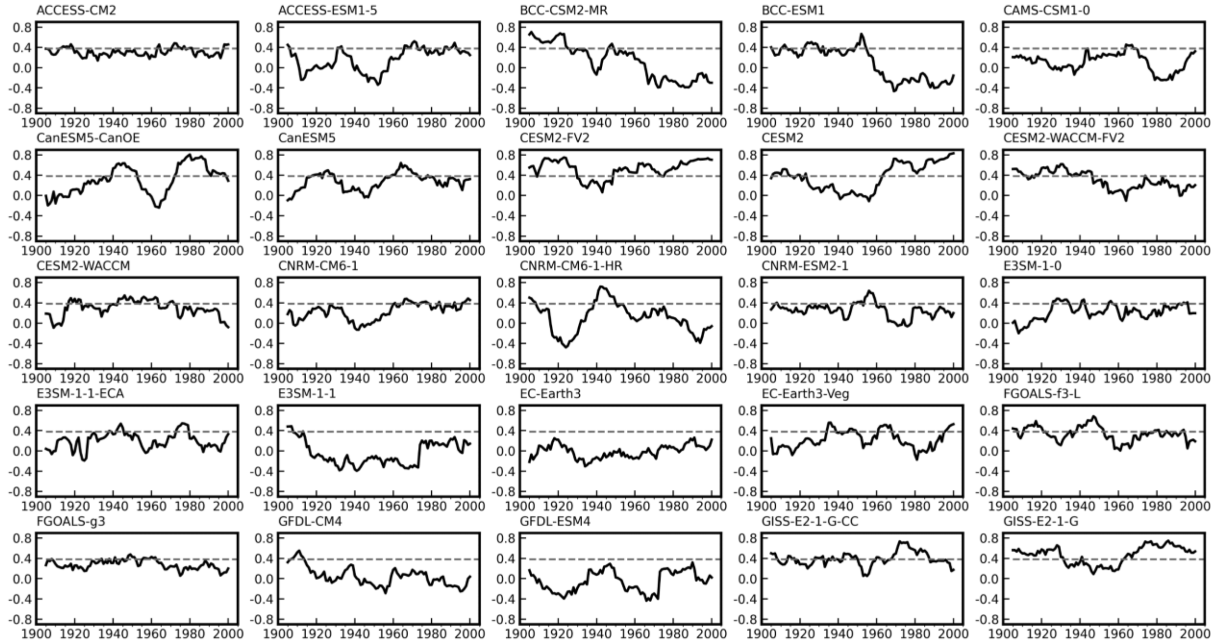


**Supplementary Fig. 3 Temporal response of precipitation (unit: mm/day) to El Niño.** 19-yr sliding correlation of DJF(0) Niño3.4 index and MAM(1) precipitation over CA for historical experiments of 45 CMIP6 models. The dashed lines denote the 90% confidence levels.

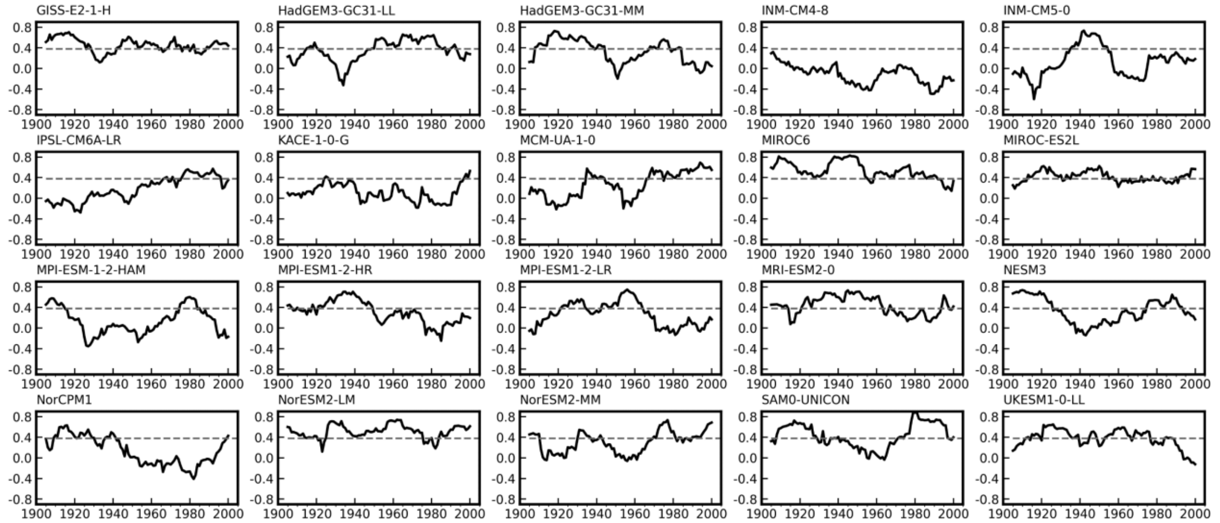


**Continued** Supplementary Fig. 3.

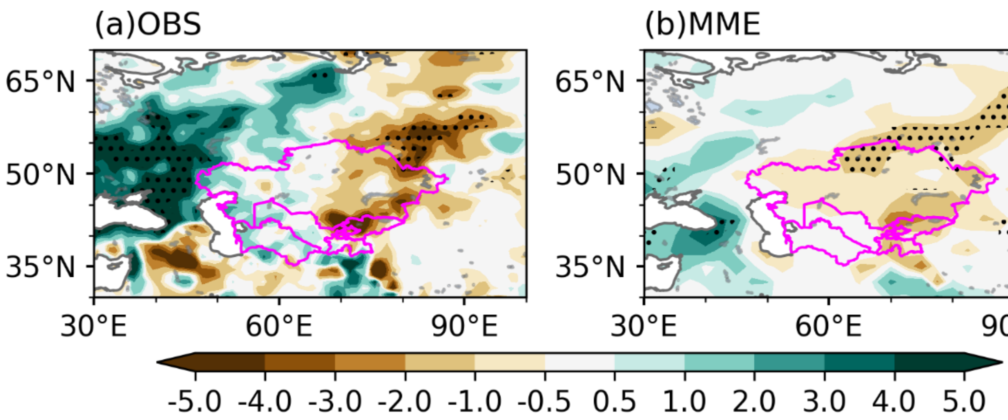


**Supplementary Fig. 4 Response of precipitation (unit: mm/day) to North Atlantic SST anomalies.** (a) Regression of MAM(1) precipitation with NAI in the observations. (b) Same as (a), but for MME. The dots denote the 90% confidence level in the observation and 80% consistency in models.

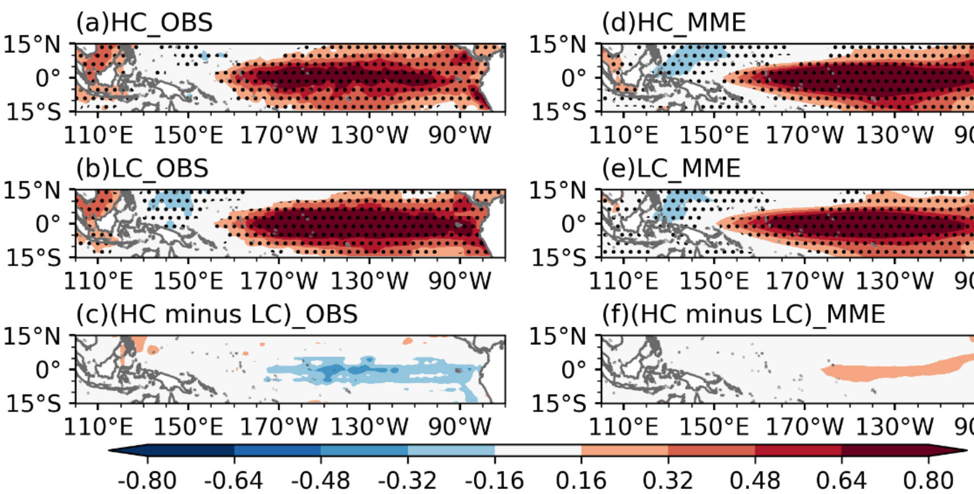


**Supplementary Fig. 5 Response of tropical Pacific SST (unit: K) to El Niño.** Regression of DJF(0) SST with DJF(0) normalized Niño3.4 index for (a) HC period and (b) LC period in the observation. (c) The difference between (a) and (b). (d–f) Same as (a–c), but for MME. The dots denote the 90% confidence level in the observation and 80% consistency in models.

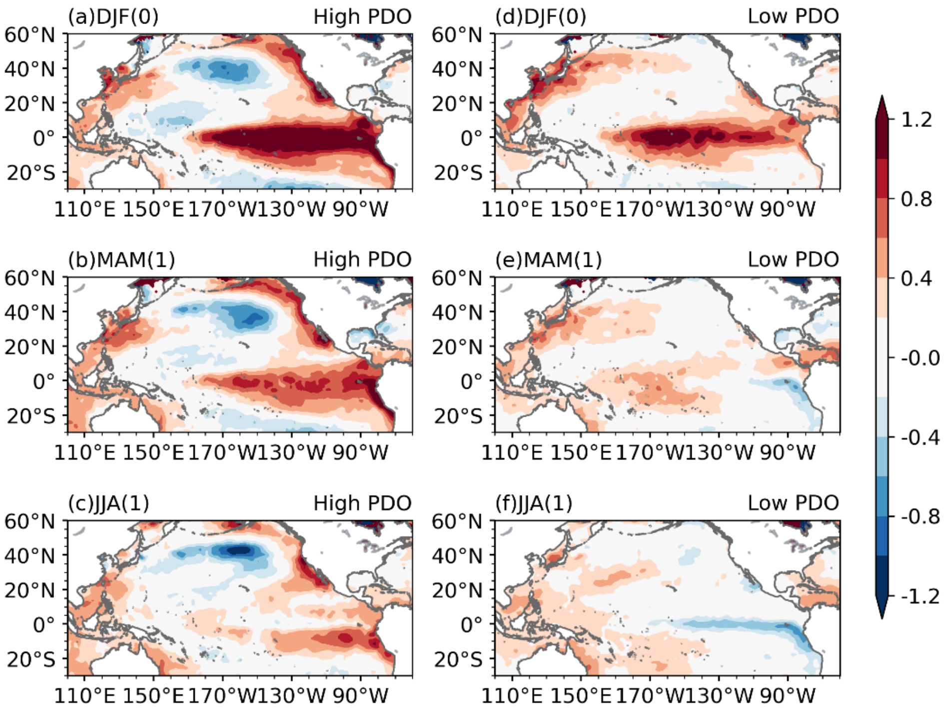


**Supplementary Fig. 6 Response of North Pacific SST (unit: K) to PDO.** Composite SST anomalies for the El Niño decaying years in (a) preceding winter DJF(0), (b) spring MAM(1) and summer JJA(1) during the positive PDO phases. (d–f) Same as (a–c), but for the negative phase of the PDO.